Inorg. Chem. **2007**, *46*, 8126–8128

Heterometallic Cubane Single-Molecule Magnets

Patrick L. Feng,[†] Christopher C. Beedle,[†] Wolfgang Wernsdorfer,[‡] Changhyun Koo,[§] Motohiro Nakano,[||] Stephen Hill,[§] and David N. Hendrickson*,[†]

Department of Chemistry and Biochemistry, University of California, San Diego, La Jolla, California 92093-0358, Institut Néel, CNRS, BP 166, Grenoble Cedex 9, France, Department of Physics, University of Florida, Gainesville, Florida 32611, and Division of Applied Chemistry, Osaka University, Suita, Osaka 565-0871, Japan

Received June 20, 2007

Two new heterometallic cubane molecules have been synthesized. High-frequency electron paramagnetic resonance and magnetization measurements indicate that $[Mn_3Ni(hmp)_3O(N_3)_3(C_7H_5O_2)_3]$ (**1**) displays a well-isolated $S = 5$ ground state ($\Delta E > 120$ K), with $g = 2.0$, $D = -0.23$ cm^{-1}, and ferromagnetic Mn–Mn exchange interactions competing with antiferromagnetic Ni–Mn interactions. $[Mn_3Zn(hmp)_3O(N_3)_3(C_3H_5O_2)_3]$ (**2**) possesses a $S = 6$ ground state ($\Delta E > 105$ K), with $g = 2.0$, $D = -0.14$ cm^{-1}, and ferromagnetic Mn–Mn exchange interactions. Magnetization vs magnetic field data for oriented single crystals of **1** and **2** indicate that both complexes are single-molecule magnets.

High-valent manganese complexes have been widely studied in the past decade because of their interesting magnetic properties and relationship to the oxygen-evolving center of photosystem II.[1−4] $Mn^{IV}Mn_3^{III}$ cubane complexes have been found to be of particular interest because they have a $S = {}^9/_2$ ground state that is well separated from excited states and function as single-molecule magnets (SMMs). These half-integer Mn_4 SMMs have been employed to demonstrate numerous phenomena such as spin frustration,[3] exchange bias in a supramolecular dimer,[5] the spin-parity effect,[6] insight into quantum coherence,[7] and the spin-parity effect.[8] Through the introduction of heterometal spins, it is possible to affect the magnetic anisotropy, spin ground state, and magnetic exchange interactions within SMMs.[9−13] Because these $Mn^{IV}Mn_3^{III}$ cubane complexes have served as a cornerstone in the study of the quantum effects in magnetization dynamics of nanomagnets, it has been of interest to modify the structure of this cubane complex by replacing one or more of the metal ions. Such modifications may provide the means to covalently interconnect two such cubane SMMs.

Herein we report two distorted heterometallic cubanes with the formulas $[Mn_3Ni(hmp)_3O(N_3)_3(C_7H_5O_2)_3]\cdot 2CHCl_3$ (**1**; Figure 1) and $[Mn_3Zn(hmp)_3O(N_3)_3(C_3H_5O_2)_3]\cdot 2CHCl_3$ (**2**).[14] Both complexes possess the same $[Mn_3XO_4]^{6+}$ cubane core structure but differ in the divalent metal ion and the nature of the carboxylate ligands.

Complexes **1** and **2** crystallize in the trigonal space group *R*3*c*. The metallic cores are composed of a triangle of Mn^{III} ions and a M^{II} ion (M = Ni in **1** and Zn in **2**) residing above the basal Mn^{III} plane. These designations were made on the basis of bond valence sum calculations and the presence of Jahn−Teller (JT) distortions. Projections of the individual-ion JT axes (O1−Mn1−O4) lead to a net axial anisotropy orthogonal to the Mn_3 plane. Three μ_3-alkoxo bridges mediate $Mn^{III}-M^{II}$ interactions, and a μ_3-oxo bridges the three Mn^{III} ions. The remaining coordination environments are completed by $3hmp^-$, $3N_3^-$, and three carboxylate ligands, where hmp^- is the anion of 2-pyridinemethanol.

* To whom correspondence should be addressed. E-mail: dhendrickson@ucsd.edu. Fax: 858-534-5383.
[†] University of California, San Diego.
[‡] Institut Néel.
[§] University of Florida, Gainesville.
[||] Osaka University.

(1) Aubin, S. M. J.; Dilley, N. R.; Pardi, L.; Krzystek, J.; Wemple, M. W.; Maple, M. B.; Brunel, L. C.; Christou, G.; Hendrickson, D. N. *J. Am. Chem. Soc.* **1998**, *120*, 4991.
(2) Ferreira, K. N.; Iverson, T. M.; Maghlaoui, K.; Barber, J.; Iwata, S. *Science* **2004**, *303*, 1831.
(3) Hendrickson, D. N.; Christou, G.; Schmitt, E. A.; Libby, E.; Bashkin, J. S.; Wang, L.; Streib, W. E. *J. Am. Chem. Soc.* **1992**, *114*, 2455.
(4) Ruettinger, W. F.; Dismukes, G. C. *Inorg. Chem.* **2000**, *39*, 1021.
(5) Wernsdorfer, W.; Aliaga-Alcalde, N.; Hendrickson, D. N.; Christou, G. *Nature* **2002**, *416*, 406.
(6) Wernsdorfer, W.; Bhaduri, S.; Tiron, R.; Hendrickson, D. N.; Christou, G. *Phys. Rev. Lett.* **2002**, *89*, 197201.
(7) Hill, S.; Edwards, E. S.; Aliaga-Alcalde, N.; Christou, G. *Science* **2003**, *302*, 1015.
(8) Wernsdorfer, W.; Bhaduri, S.; Boskovic, C.; Christou, G.; Hendrickson, D. N. *Phys. Rev. B* **2002**, *65*, 180403.
(9) Oshio, H.; Nihei, M.; Koizumi, S.; Shiga, T.; Nojiri, H.; Nakano, M.; Shirakawa, N.; Akatsu, M. *J. Am. Chem. Soc.* **2005**, *127*, 4568.
(10) Christou, G.; Gatteschi, D.; Hendrickson, D. N.; Sessoli, R. *MRS Bull.* **2000**, *25*, 66.
(11) Osa, S.; Kido, T.; Matsumoto, N.; Re, N.; Pochaba, A.; Mrozinski, J. *J. Am. Chem. Soc.* **2004**, *126*, 420.
(12) Oshio, H.; Nihei, M.; Yoshida, A.; Nojiri, H.; Nakano, M.; Yamaguchi, A.; Ishiomoto, H. *Chem.—Eur. J.* **2004**, *11*, 843.
(13) Schelter, E. J.; Karadas, F.; Avendano, C.; Prosvirin, A. V.; Wernsdorfer, W.; Dunbar, K. R. *J. Am. Chem. Soc.* **2007**, *129*, 8139.
(14) Complex **1** was synthesized by adding $MnCl_2\cdot 4H_2O$ (0.50 g, 2.04 mmol) and $Ni(NO_3)_2\cdot 4H_2O$ (0.50 g, 2.01 mmol) to a $CHCl_3$ mixture of benzoic acid (0.25 g, 2.04 mmol), (hydroxymethyl)pyridine (0.44 mL, 4.62 mmol), NBu_4MnO_4 (0.092 g, 0.25 mmol), and NaN_3 (0.13 g, 2.05 mmol). The solution was stirred, filtered, and layered with Et_2O. After 3 weeks, very dark-red crystals were collected in 50% yield. A similar procedure was followed to obtain **2**.

10.1021/ic7012107 CCC: $37.00
Published on Web 09/07/2007

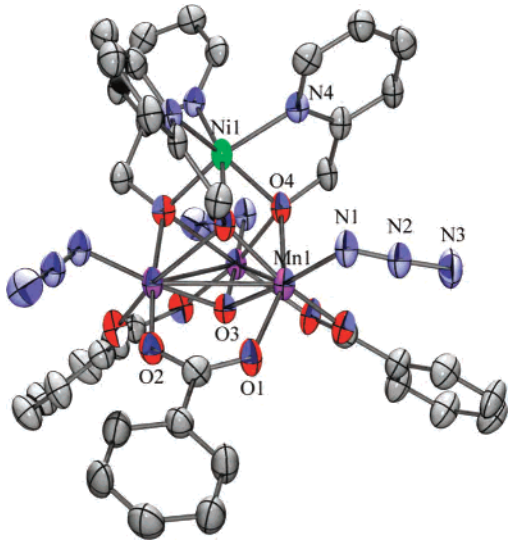

Figure 1. ORTEP diagram of **1**. Thermal ellipsoids are at 50% probability. **2** retains the same core structure but with Zn^{2+} replacing Ni^{2+}.

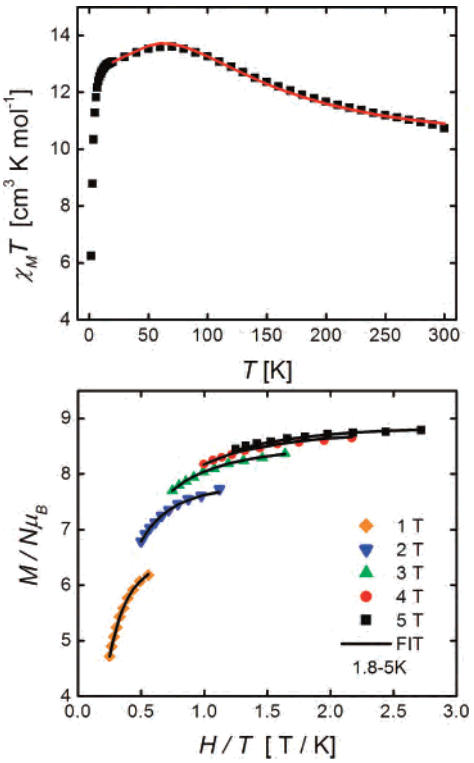

Figure 2. $\chi_m T$ vs T (top) plot and field dependence of magnetization at the fields indicated (bottom) for **1**. The solid lines are the best fits using values given in the text.

Magnetic susceptibility measurements were carried out at 1 T on a polycrystalline sample embedded in eicosane. The $\chi_m T$ vs T plot of **1** shows a room-temperature value of 10.7 $cm^3 \cdot K \cdot mol^{-1}$ that increases upon cooling to a maximum value of 13.6 cm3·K·mol^{-1} at 60 K, followed by a decrease below 60 K (Figure 2, top). The $\chi_m T$ vs T plot of **2** shows a room-temperature value of 11.3 $cm^3 \cdot K \cdot mol^{-1}$ that increases upon cooling to a maximum value of 21.0 $cm^3 \cdot K \cdot mol^{-1}$ at 16 K (Figure 3, top). To determine the spin-state distribution and exchange interactions in **1**, a Heisenberg−Dirac−van Vleck spin Hamiltonian was employed. The spin Hamiltonian

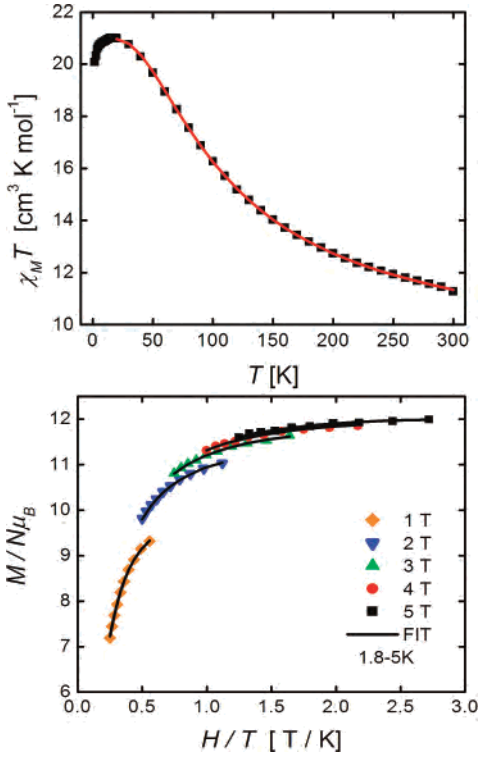

Figure 3. $\chi_m T$ vs T (top) plot and field dependence of magnetization at the fields indicated (bottom) for **2**. The solid lines are the best fits using values given in the text.

for a $Mn^{III}_3Ni^{II}$ complex with C_3 symmetry is given by eq 1

$$\hat{H} = -2J_{Ni-Mn}(\hat{S}_1\hat{S}_2 + \hat{S}_1\hat{S}_3 + \hat{S}_1\hat{S}_4) - 2J_{Mn-Mn}(\hat{S}_2\hat{S}_3 + \hat{S}_2\hat{S}_4 + \hat{S}_3\hat{S}_4) \quad (1)$$

where $S_1 = 1$ and $S_2 = S_3 = S_4 = 2$. The Kambe vector coupling method was used to determine the eigenvalue equation, where $\hat{S}_A = (\hat{S}_2 + \hat{S}_3 + \hat{S}_4)$ and $\hat{S}_T = (\hat{S}_1 + \hat{S}_A)$.

$$E(S_T,S_A) = -J_{Ni-Mn}[(S_T(S_T + 1) - S_A(S_A + 1))] - J_{Mn-Mn}[S_A(S_A + 1)] \quad (2)$$

Determination of the values of J_{Ni-Mn} and J_{Mn-Mn} for complex **1** was accomplished by substitution of these energies into the van Vleck equation. An isolated $S = 5$ ground state ($\Delta E = 122$ K) was obtained with best-fit parameters of $g = 1.9$, $J_{Ni-Mn} = -5.2$ cm^{-1}, and $J_{Mn-Mn} = 8.3$ cm^{-1}. A similar approach was followed for **2**, resulting in an isolated $S = 6$ ground state ($\Delta E = 107$ K) and parameters of $g = 2.0$ and $J_{Mn-Mn} = 7.4$ cm^{-1}.

Variable-field magnetization data were collected to confirm the spin ground state of the two complexes. Because **1** and **2** exhibit well-isolated ground states, the Hamiltonian given in eq 3 can be used, where D is the axial zero-field-

$$H = D\hat{S}_z^2 + g\mu_B\mu_0\hat{S}_zH_z \quad (3)$$

splitting (zfs) parameter, μ_B is the Bohr magneton, μ_0 is the vacuum permeability, $\hat{S}_z$ is the easy-axis spin operator, and H_z is the applied field. The best fit for **1** (Figure 2, bottom) gave parameters of $S = 5$, $g = 1.9$, and $D = -0.22$ cm^{-1}.

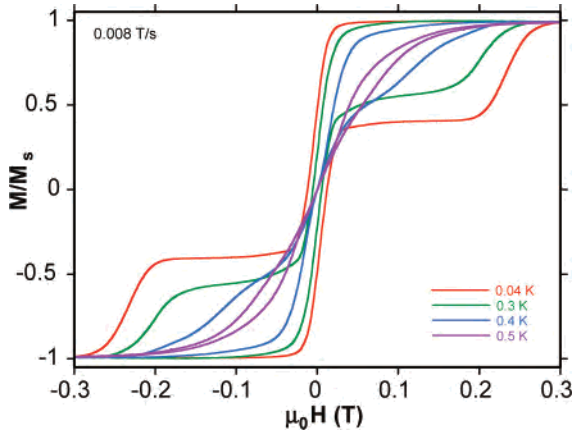

Figure 4. Temperature-dependent hysteresis loop measurements for a single crystal of **1**. The magnetization is normalized by the saturation value M_s.

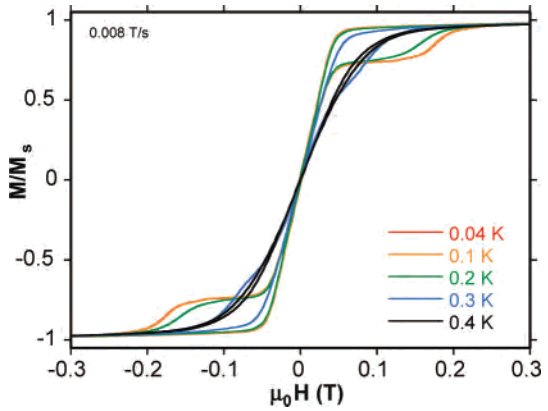

Figure 5. Temperature-dependent hysteresis loop measurements for a single crystal of **2**. The magnetization is normalized by the saturation value M_s.

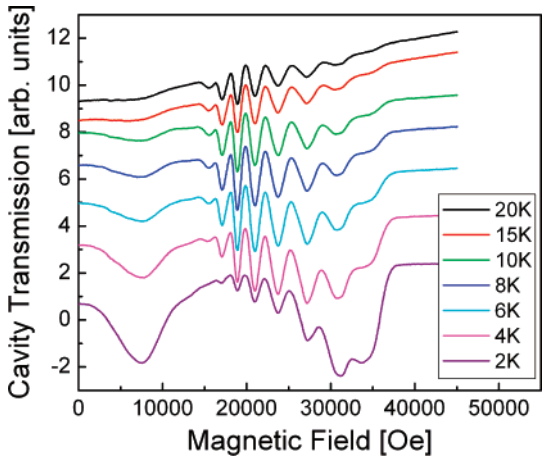

Figure 6. Hard-plane temperature-dependent spectra for **1** collected at 59.9 GHz.

The best fit for **2** gave $S = 6$, $g = 2.0$, and $D = -0.14$ cm^{-1} (Figure 3, bottom).

Alternating current (ac) magnetic susceptibility measurements in a zero direct current field were performed on polycrystalline samples from 5.0 to 1.8 K with a 3.0 G ac field oscillating at 250−1000 Hz. The onset of a frequency-dependent out-of-phase signal below 3 K suggests that complex **1** is a SMM. To further probe this possibility, single-crystal hysteresis loop measurements were performed using a micro-SQUID array.[15] The resulting hysteresis loops, shown in Figures 4 and 5 for complexes **1** and **2**, respectively, are indicative of SMMs, as indicated by the temperature dependence of the coercivity. In both cases, after magnetization saturation in a field, reduction of the field leads to a pronounced step at $H = 0$, whereupon reversal of the field direction leads to a second step. The separation between vertical steps corresponds to D. There is clearly a very rapid rate of tunneling of the magnetization direction present in complex **1** and an even faster tunneling in complex **2**. The $Mn^{IV}Mn_3^{III}$ SMMs exhibit a slower magnetization tunneling because they have a half-integer spin ground state.[8]

High-frequency electron paramagnetic resonance (HFEPR) experiments were carried out on a single crystal of **1** in order to obtain the spin of the ground state (S), and the sign and magnitude of the zfs parameter (D), using previously published methods.[16] Figure 6 illustrates the temperature dependence of the hard-plane (xy) spectra for **1** collected from 2 to 20 K at 59.9 GHz and clearly indicates that the sign of D is negative (increased intensity for high-field transitions at low temperatures). HFEPR data were collected at several frequencies in two orthogonal planes. The resonance fields for both orientations were fit, giving the following zfs parameters: $S = 5$, $g_z = 2.02$, $D = -0.23$ cm^{-1}, and $B_4^0 = -5.7 \times 10^{-6}$ cm^{-1}. These fitting parameters are in good agreement with the parameters calculated from theoretical fits of reduced magnetization ($g = 1.9$ and $D = -0.22$ cm^{-1}) and magnetization hysteresis data ($D = -0.24$ cm^{-1}).

Two new heterometallic SMMs that exhibit well-isolated integer spin ground states have been synthesized. These molecules possess a triangle of ferromagnetically coupled Mn^{III} ions and exhibit fast magnetization tunneling. The large energy separation between the ground and first excited spin states leads to S and M_s as good quantum numbers. This is often not the case in manganese chemistry, making **1** and **2** very attractive for fundamental, detailed studies of magnetic exchange and quantum phenomena. By variation of the divalent metal ion and carboxylate ligands, tuning of the spin ground state, axial anisotropy, pairwise exchange interactions, and intermolecular exchange interactions can be achieved. Following similar synthetic methods, other heterometallic cubane and bridged cubane molecules have been made. These complexes possess varying combinations of manganese oxidation states, leading to integer and half-integer spin ground states. Investigation of these molecules is currently underway and will be reported in a future publication.

Acknowledgment. This work was supported by the National Science Foundation.

Supporting Information Available: Crystallographic information in CIF format and ac susceptibility data. This material is available free of charge via the Internet at http://pubs.acs.org. CCDC nos. 651291 and 651292 contain the supplementary crystallographic data for this paper. These data can be obtained free of charge from The Cambridge Crystallographic Data Centre via www.ccdc.cam.ac.uk/data_request/cif or CCDC, 12 Union Road, Cambridge CB2 1EZ, U.K. (tel +441223 336408, fax +44 1223 336033).

IC7012107

(15) Wernsdorfer, W. *Adv. Chem. Phys.* **2001**, *118*, 99.
(16) Takahashi, S.; Hill, S. *Rev. Sci. Instrum.* **2005**, *76*, 023114.